

Neutrino oscillations with three flavors in matter of varying density

T. Ohlsson^{1,2,a}, H. Snellman^{2,b}

¹ Institut für Theoretische Physik, Physik Department, Technische Universität München, James-Frank-Strasse, 85748 Garching bei München, Germany

² Division of Mathematical Physics, Theoretical Physics, Department of Physics, Royal Institute of Technology, 100 44 Stockholm, Sweden

Received: 23 March 2001 /

Published online: 8 June 2001 – © Springer-Verlag / Società Italiana di Fisica 2001

Abstract. In this paper, we discuss the evolution operator and the transition probabilities expressed as functions of the vacuum mass squared differences, the vacuum mixing angles, and the matter density parameter for three flavor neutrino oscillations in matter of varying density in the plane wave approximation. The applications of this to neutrino oscillations in a model of the earth’s matter density profile, step function matter density profiles, constant matter density profiles, linear matter density profiles, and finally in a model of the sun’s matter density profile are discussed. We show that for matter density profiles which do not fluctuate too much, the total evolution operator consisting of n operators can be replaced by one single evolution operator in the semi-classical approximation.

1 Introduction

In previous papers [1,2], we have given analytic expressions for the three flavor neutrino oscillation evolution operator and the transition probabilities in presence of constant matter densities expressed in the vacuum mixing matrix elements and the neutrino energies or masses, i.e., incorporating the so-called Mikheyev–Smirnov–Wolfenstein (MSW) effect [3,4]. Here we will discuss the application of this to realistic matter density variations in a “semi-classical” approximation based on our previous results. This allows a simple and efficient calculation to be made of neutrino oscillations in media of varying densities. We compare this approximate formula with a numerical simulation in a multi-step model. We will as before assume that the CP phase δ is equal to zero. Thus, the neutrino mixing matrix is real. The semi-classical approximation for three neutrino flavors, we believe, is a unique part of our investigation.

Previous work on models for three flavor neutrino oscillations in matter for constant matter density includes works of Barger et al. [5], Kim and Sze [6], and Zaglauer and Schwarzer [7]. Approximate solutions for three flavor neutrino oscillations in matter have been presented by Kuo and Pantaleone [8] and Joshipura and Murthy [9]. Approximate treatments have also been done by Toshev and Petcov [10]. D’Olivio and Oteo have made contribu-

tions by using an approximative Magnus expansion for the time evolution operator [11]. Extensive numerical investigations for matter enhanced three neutrino oscillations have been made by Fogli et al. [12]. Studies of neutrino oscillations in earth has been performed by several authors [13–18].

Neutrino oscillations for matter with linearly varying density have been treated by Petcov [19] and Lehmann et al. [20]. Osland and Wu [21] have also solved the case for exponentially varying density. Matter enhanced two flavor neutrino oscillations with an arbitrary monotonic matter density profile have been studied by Balantekin and Beacom [22] using a uniform semi-classical approximation. See also Fishbane et al. [23] for two flavor neutrino oscillations in matter of varying density.

2 The evolution operator in presence of matter

Let the flavor state basis and mass eigenstate basis be denoted by $\mathcal{B}_f \equiv \{|\nu_\alpha\rangle\}_{\alpha=e,\mu,\tau}$ and $\mathcal{B}_m \equiv \{|\nu_a\rangle\}_{a=1}^3$, respectively. Then the flavor states $|\nu_\alpha\rangle \in \mathcal{B}_f$ can be obtained as a superposition of the mass eigenstates $|\nu_a\rangle \in \mathcal{B}_m$, or vice versa. The bases \mathcal{B}_f and \mathcal{B}_m are of course just two different representations of the same Hilbert space.

In the present analysis, we will use the plane wave approximation to describe neutrino oscillations. In this approximation, a neutrino flavor state $|\nu_\alpha\rangle$ is a linear combination of neutrino mass eigenstates $|\nu_a\rangle$ ’s such that [24]

^a e-mail: tohlsson@physik.tu-muenchen.de or tommy@theophys.kth.se

^b e-mail: snell@theophys.kth.se

$$|\nu_\alpha\rangle = \sum_{a=1}^3 U_{\alpha a}^* |\nu_a\rangle, \quad (1)$$

where $\alpha = e, \mu, \tau$. In what follows, we will use the shorthand notations $|\alpha\rangle \equiv |\nu_\alpha\rangle$ and $|a\rangle \equiv |\nu_a\rangle$ for the flavor states and the mass eigenstates, respectively.

The components of a state ψ in flavor basis and mass basis, respectively, are related to each other by

$$\psi_f = U\psi_m, \quad (2)$$

where

$$\psi_f \equiv (\psi_\alpha) \equiv \begin{pmatrix} \psi_e \\ \psi_\mu \\ \psi_\tau \end{pmatrix} \in \mathcal{B}_f$$

and

$$\psi_m \equiv (\psi_a) \equiv \begin{pmatrix} \psi_1 \\ \psi_2 \\ \psi_3 \end{pmatrix} \in \mathcal{B}_m.$$

A convenient parameterization for $U = U(\theta_1, \theta_2, \theta_3)$ is given by [25]

$$U = \begin{pmatrix} C_2 C_3 & S_3 C_2 & S_2 \\ -S_3 C_1 - S_1 S_2 C_3 & C_1 C_3 - S_1 S_2 S_3 & S_1 C_2 \\ S_1 S_3 - S_2 C_1 C_3 & -S_1 C_3 - S_2 S_3 C_1 & C_1 C_2 \end{pmatrix}, \quad (3)$$

where $S_i \equiv \sin \theta_i$ and $C_i \equiv \cos \theta_i$ for $i = 1, 2, 3$. This is the standard representation of the neutrino mixing matrix. The quantities θ_i , where $i = 1, 2, 3$, are the vacuum mixing angles. Since we have put the CP phase equal to zero in the neutrino mixing matrix, this means that $U_{\alpha a}^* = U_{\alpha a}$ for $\alpha = e, \mu, \tau$ and $a = 1, 2, 3$.

In the mass basis, the Hamiltonian \mathcal{H} for the propagation of the neutrinos in vacuum is diagonal and is given by

$$H_m = \begin{pmatrix} E_1 & 0 & 0 \\ 0 & E_2 & 0 \\ 0 & 0 & E_3 \end{pmatrix}, \quad (4)$$

where $E_a = (m_a^2 + \mathbf{p}^2)^{1/2}$, $a = 1, 2, 3$, are the energies of the neutrino mass eigenstates $|a\rangle$, $a = 1, 2, 3$ with masses m_a , $a = 1, 2, 3$. We will assume the three-momentum \mathbf{p} to be the same for all mass eigenstates.

When neutrinos propagate in ordinary matter, there is an additional term in the Hamiltonian \mathcal{H} coming from the presence of electrons in matter [4]. This term, the potential term, is diagonal in flavor basis and is given by

$$V_f = A \begin{pmatrix} 1 & 0 & 0 \\ 0 & 0 & 0 \\ 0 & 0 & 0 \end{pmatrix} \equiv AK_f, \quad (5)$$

where

$$A \equiv A(r) = \pm \sqrt{2} G_F N_e(r) \simeq \pm \frac{1}{\sqrt{2}} G_F \frac{1}{m_N} \rho(r)$$

is the matter density parameter and K_f is the projector in the flavor basis on the electron neutrinos. Here G_F is the Fermi weak coupling constant, N_e is the electron density, m_N is the nucleon mass, and ρ is the matter density. The sign of the matter density parameter depends on whether we deal with neutrinos (+) or antineutrinos (-). In the mass basis, this piece of the Hamiltonian is $V_m = U^{-1} V_f U$, where U is again the neutrino mixing matrix.

In the case when the neutrinos propagate through matter, as here, the Hamiltonian is not diagonal in either the mass basis or the flavor basis, and we have to calculate the evolution operator $U_f(t)$ or $U_f(L) \equiv e^{-i\mathcal{H}_f L} = U e^{-i\mathcal{H}_m L} U^{-1}$ if we set $t = L$ (L is the traveling (propagation) path length of the neutrinos.).

To do so it is convenient to introduce the traceless real symmetric matrix T defined by $T \equiv \mathcal{H}_m - (\text{tr} \mathcal{H}_m) I / 3$. The trace of the Hamiltonian in mass basis $\mathcal{H}_m \equiv H_m + U^{-1} V_f U$ is $\text{tr} \mathcal{H}_m = E_1 + E_2 + E_3 + A$, and the matrix T can then be written as (see (6) on top of the next page) where $E_{ab} \equiv E_a - E_b$. Of the six antisymmetric quantities E_{ab} , where $a, b = 1, 2, 3$ and $a \neq b$, only two are linearly independent, since the E_{ab} 's fulfill the relations $E_{ba} = -E_{ab}$ and $E_{12} + E_{23} + E_{31} = 0$ ¹. This means that the evolution operator in the mass basis can be written as [1, 2]

$$U_m(L) \equiv e^{-i\mathcal{H}_m L} = \phi e^{-iLT} \quad (7)$$

$$= \phi \sum_{a=1}^3 e^{-iL\lambda_a} \frac{1}{3\lambda_a^2 + c_1} [(\lambda_a^2 + c_1)I + \lambda_a T + T^2],$$

where $\phi \equiv e^{-iL(\text{tr} \mathcal{H}_m)I/3}$, λ_a , $a = 1, 2, 3$, are the eigenvalues of the matrix T , and I is the 3×3 identity matrix². The coefficients c_0 , c_1 , and c_2 are all real and the eigenvalues λ_a , $a = 1, 2, 3$, can be expressed in closed form in terms of these [1, 2].

The evolution operator for the neutrinos in flavor basis is thus given by

$$U_f(L) = e^{-i\mathcal{H}_f L} = U e^{-i\mathcal{H}_m L} U^{-1} \quad (8)$$

$$= \phi \sum_{a=1}^3 e^{-iL\lambda_a} \frac{1}{3\lambda_a^2 + c_1} [(\lambda_a^2 + c_1)I + \lambda_a \tilde{T} + \tilde{T}^2],$$

¹ Later, we will use the usual (vacuum) mass squared differences Δm_{21}^2 and Δm_{32}^2 , instead of E_{21} and E_{32} , which are related to each other by $\Delta m_{21}^2 = 2E_\nu E_{21}$ and $\Delta m_{32}^2 \simeq 2E_\nu E_{32}$, where E_ν is the neutrino energy

² Using Cayley–Hamilton's theorem, the exponential of a matrix M , $e^M = \sum_{n=0}^{\infty} \frac{1}{n!} M^n$ (infinite series), can be written as $e^M = \sum_{n=0}^{N-1} a_n M^n$ (finite series, N is the dimension of M), where a_n ($n = 0, 1, \dots, N-1$) are some coefficients to be determined. In this case, since $N = 3$ (the dimension of T is three), this means that we have $e^{-iLT} = a_0 I - ia_1 LT - a_2 L^2 T^2$, i.e., there are no higher power terms of T in e^{-iLT} than that of order two

$$T = (T_{ab}) = \begin{pmatrix} AU_{e1}^2 - \frac{1}{3}A + \frac{1}{3}(E_{12} + E_{13}) & AU_{e1}U_{e2} & AU_{e1}U_{e3} \\ AU_{e1}U_{e2} & AU_{e2}^2 - \frac{1}{3}A + \frac{1}{3}(E_{21} + E_{23}) & AU_{e2}U_{e3} \\ AU_{e1}U_{e3} & AU_{e2}U_{e3} & AU_{e3}^2 - \frac{1}{3}A + \frac{1}{3}(E_{31} + E_{32}) \end{pmatrix}, \quad (6)$$

where $\tilde{T} \equiv UTU^{-1}$. Equation (8) is our final expression for $U_f(L)$.

Since $\mathcal{H}_f = U\mathcal{H}_mU^{-1}$, it is clear that $\tilde{T} = \mathcal{H}_f - (\text{tr}\mathcal{H}_f)I/3 = \mathcal{H}_f - (\text{tr}\mathcal{H}_m)I/3$ due to the invariance of the trace under transformation of U . In fact, the characteristic equation is also invariant under transformation of U and therefore so are the coefficients c_0, c_1, c_2 , and the eigenvalues $\lambda_1, \lambda_2, \lambda_3$. However, the expression for \mathcal{H}_f is much more complicated than that for \mathcal{H}_m , which is the reason why we work with \mathcal{H}_m instead of \mathcal{H}_f .

The formula (8) expresses the time (or L) evolution directly in terms of the mass squared differences and the vacuum mixing angles without introducing any auxiliary matter mixing angles. By dividing the density variation in small, approximately constant segments, and using this formula repeatedly in each segment, we can numerically study neutrino oscillations in matter with varying density. We will use this method as a standard test for the semi-classical approximation to the evolution operator that we study below.

3 The semi-classical approximation

The formula given in (8) is the evolution operator in flavor basis for constant matter density. To handle the case of varying matter density, let us divide the distance L from the source to the detector into N equidistant parts and put the index k on the eigenvalues λ_a^k , where $a = 1, 2, 3$ denote the three mass eigenstates. For any matter density profile $\rho(r)$ we first make this profile discrete and introduce ρ_k as the matter density in the interval $r_{k-1} \leq r \leq r_k$, where k varies from 1 to N with $r_0 = 0$ and $r_N = L$. The length of each segment is then $\Delta r_k = r_k - r_{k-1} = L/N$. The evolution operator in mass basis from 0 to L can then be written as the ordered product

$$U_m(L) = U_m(r_N - r_{N-1})U_m(r_{N-1} - r_{N-2}) \dots \dots U_m(r_2 - r_1)U_m(r_1 - r_0). \quad (9)$$

Note that the order of the $U_m(r_k - r_{k-1})$'s is important, since these operators do not in general commute.

When N is large, each step is small and the exponent in the evolution operator $U_m(r_k - r_{k-1}) = U_m(\Delta r_k)$ is small. We can then approximate this operator with

$$U_m(\Delta r_k) \simeq e^{-i\Delta r_k \mathcal{H}_m^k}, \quad (10)$$

where $\mathcal{H}_m^k \equiv H_m + A_k K_m$ and $A_k \propto \rho_k$. Inserting this into (9) gives

$$U_m(L) \simeq e^{-i\Delta r_N \mathcal{H}_m^N} e^{-i\Delta r_{N-1} \mathcal{H}_m^{N-1}} \dots e^{-i\Delta r_2 \mathcal{H}_m^2} e^{-i\Delta r_1 \mathcal{H}_m^1}. \quad (11)$$

Since the \mathcal{H}_m^k 's do not commute, the higher order terms have to be calculated with the time-ordering (here rather r -ordering) operator. However, here we will at first be satisfied with the lowest order result, which we call the *semi-classical approximation*. In this approximation, we retain only the terms proportional to $\Delta r_k = L/N$, and thus, neglect the noncommutativity of the \mathcal{H}_m^k 's for different k 's. We can thus write

$$U_m(L) \simeq e^{-i\sum_{k=1}^N \frac{L}{N} \mathcal{H}_m^k}. \quad (12)$$

In the limit $N \rightarrow \infty$, this gives the integral formula

$$U_m(L) = e^{-i\int_0^L \mathcal{H}_m(r)dr} = \phi(L)e^{-i\int_0^L T(r)dr}, \quad (13)$$

where $T(r)$ is the traceless part of the Hamiltonian corresponding to the electron density at position r between 0 and L and $\phi(L)$ is the phase factor coming from the trace.

For further discussion it is often convenient to retain the original form of the Hamiltonian and to use $\mathcal{H}_m = H_m + AU^{-1}K_fU$ rather than T . Thus, when $A = A(r)$, we obtain

$$\int_0^L \mathcal{H}_m(r)dr = L(H_m + \bar{A}(L)K_m), \quad (14)$$

where

$$\bar{A}(L) \equiv \frac{1}{L} \int_0^L A(r)dr$$

is the average matter density along the baseline L and

$$K_m \equiv U^{-1}K_fU,$$

which means that the evolution operator in the mass basis can be written as

$$U_m(L) = e^{-iL(H_m + \bar{A}(L)K_m)} \equiv \bar{\phi}e^{-iL\bar{T}}, \quad (15)$$

where $\bar{\phi} \equiv e^{-iL(\text{tr}\bar{\mathcal{H}}_m)/3}$, $\bar{T} \equiv \bar{\mathcal{H}}_m - (\text{tr}\bar{\mathcal{H}}_m)I/3$, and $\bar{\mathcal{H}}_m \equiv H_m + \bar{A}(L)K_m$.

For this case we can thus use the previous expression for $T = \mathcal{H}_m - (\text{tr}\mathcal{H}_m)I/3$ by simply replacing A with $\bar{A}(r)$ and then pass to the flavor basis by using the U transformation, i.e., $\tilde{T} = UTU^{-1}$.

Thus, for any L we can use the spectral decomposition theorem and we find that

$$U_f(L) = \phi(L) \sum_{a=1}^3 e^{-iL\lambda_a(L)} P_a(L), \quad (16)$$

where $\lambda_a(L)$ is the a th eigenvalue of $T(L)$ (or $\tilde{T}(L)$) and

$$P_a(L) = \frac{1}{3\lambda_a^2(L) + c_1(L)} \times \left[(\lambda_a^2(L) + c_1(L))I + \lambda_a(L)\tilde{T}(L) + \tilde{T}^2(L) \right] \quad (17)$$

is the projection operator. Everything here is of course L -dependent, since the operator is L -dependent and therefore also the eigenvalues. The phase factor is $\phi(L) = e^{-iL(\text{tr}\mathcal{H}_f(L))/3} = e^{-iL(\text{tr}\mathcal{H}_m(L))/3}$.

In the case of a linear matter density of the form $A(r) = A + Br$, we obtain $\bar{A}(r) = A + Br/2$. Similarly, in the case of a step function like matter density, relevant to the matter distribution of the earth, we have

$$A(r) = \begin{cases} A_1, & 0 \leq r \leq L_1, \\ A_2, & L_1 \leq r \leq L_1 + L_2, \\ A_1, & L_1 + L_2 \leq r \leq 2L_1 + L_2, \end{cases}$$

where $2L_1 + L_2 \equiv L$, which leads to

$$\bar{A}(r) = \begin{cases} A_1, & 0 \leq r \leq L_1, \\ A_2 \left(1 - \frac{L_1}{r}\right) + A_1 \frac{L_1}{r}, & L_1 \leq r \leq L_1 + L_2, \\ A_1 \left(1 - \frac{L_2}{r}\right) + A_2 \frac{L_2}{r}, & L_1 + L_2 \leq r \leq 2L_1 + L_2. \end{cases} \quad (18)$$

Finally, in the case of an exponentially decreasing matter density $A(r) = Ae^{-r/r_0}$, where A and r_0 are parameters relevant to the matter distribution of the sun, we obtain

$$\bar{A}(r) = A \frac{r_0}{r} \left(1 - e^{-r/r_0}\right). \quad (19)$$

We can see here that in the semi-classical approximation the influence of the density \bar{A} decays as $1/L$ with distance L from the matter. The evolution should therefore be continued with the vacuum evolution operator as soon as the neutrinos leave the matter region.

4 Digression on the semi-classical approximation

Let us consider the semi-classical (s.c.) evolution operator further. It can be written as

$$U(r)_m^{\text{s.c.}} = e^{-i\mathcal{H}_m^{(1)}(r)}, \quad (20)$$

where

$$\mathcal{H}_m^{(1)}(r) \equiv H_m r + A^{(1)}(r)K_m.$$

Here $A^{(1)}(r) \equiv \int_0^r A(s)ds$. Now, the equation of motion for the full evolution operator U_m is

$$i \frac{d}{dr} U_m(r) = \mathcal{H}_m(r) U_m(r). \quad (21)$$

This can be integrated to give the equation

$$U_m(r) = 1 - i \int_0^r \mathcal{H}_m(s) U_m(s) ds. \quad (22)$$

Upon differentiating the semi-classical evolution operator above, we see that, although

$$\frac{d}{dr} \mathcal{H}_m^{(1)}(r) = \mathcal{H}_m(r) = H_m + A(r)K_m, \quad (23)$$

we can equate $i(d/dr)U_m^{\text{s.c.}}(r)$ with $\mathcal{H}_m(r)U_m^{\text{s.c.}}(r)$ only when the commutator $[\mathcal{H}_m^{(1)}(r), \mathcal{H}_m(r)]$ can be neglected. This commutator can be calculated to be

$$[\mathcal{H}_m^{(1)}(r), \mathcal{H}_m(r)] = \int_0^r s \frac{dA}{ds}(s) ds [H_m, K_m]. \quad (24)$$

Thus, when

$$\int_0^r s \frac{dA}{ds}(s) ds = \frac{r^2}{2} \frac{dA}{ds}(\xi)$$

for $0 \leq \xi \leq r$ is small, the semi-classical approximation to the evolution operator is a good approximation to the full evolution operator. For constant matter density this is of course true. For linear matter density $A(r) = A + Br$ the coefficient B should be small, i.e., $Br \ll A$ or at least $Br < A$.

Equation (22) can be solved in a systematic way by iteration, leading to

$$U_m(r) = 1 - i \int_0^r \mathcal{H}_m(s) ds + (-i)^2 \int_0^r \mathcal{H}_m(s) \int_0^s \mathcal{H}_m(s') ds' ds + \dots \quad (25)$$

The Hamiltonian $\mathcal{H}_m(r)$ is the one given in (23). The result to second order is then given by

$$U_m(r) \simeq 1 - ir (H_m + \bar{A}(r)K_m) + (-i)^2 \frac{r^2}{2} (H_m + \bar{A}(r)K_m)^2 + (-i)^2 \frac{r^2}{2} (\bar{\bar{A}}(r) - \bar{A}(r)) [H_m, K_m], \quad (26)$$

where

$$\bar{A}(r) \equiv A^{(1)}(r)/r, \quad A^{(1)}(r) \equiv \int_0^r A(s) ds, \\ \bar{\bar{A}}(r) \equiv 2A^{(2)}(r)/r^2, \quad A^{(2)}(r) \equiv \int_0^r A^{(1)}(s) ds.$$

By inspection we see that the expression in (26) deviates from an expansion of the semi-classical approximation by the terms proportional to the commutator $[H_m, K_m]$ and higher order terms in H_m and K_m . In fact, the commutator between the Hamiltonian at different points s and s' is

$$[\mathcal{H}_m(s), \mathcal{H}_m(s')] = (A(s) - A(s')) [H_m, K_m] \\ = \frac{dA}{ds} \Big|_{s=s'} (s - s') [H_m, K_m] + \dots, \quad (27)$$

which vanishes only for $A(s) = A(s')$. This is in general true only for constant matter densities, $A(s) = A$. When

dA/ds is large, the contribution of the commutator cannot be neglected.

We can therefore sum the semi-classical approximation terms and write the solution as

$$U_m(r) = U_m^{s.c.}(r) + a_1 [H_m, K_m] + \dots, \quad (28)$$

where

$$a_1 = (-i)^2 \frac{r^2}{2} (\bar{A}(r) - \bar{A}(r))$$

and the dots represent higher order terms that vanish when the commutator $[H_m, K_m]$ is neglected. When $|\bar{A} - \bar{A}|$ is small, the correction terms are small.

5 Probability amplitudes and transition probabilities

In the previous sections, we have calculated the evolution operator in the semi-classical approximation. Below we will study the corresponding probability amplitudes and transition probabilities.

The probability amplitude $A_{\alpha\beta}$ for the $\nu_\alpha \rightarrow \nu_\beta$ transition is simply defined as the (β, α) -matrix element of the evolution operator in flavor basis, i.e.,

$$A_{\alpha\beta} \equiv \langle \beta | U_f(L) | \alpha \rangle, \quad \alpha, \beta = e, \mu, \tau. \quad (29)$$

We now consider transition probabilities for neutrino oscillations in the semi-classical approximation given by (16). Inserting (16) into (29) gives

$$A_{\alpha\beta} = \phi(L) \sum_{a=1}^3 e^{-iL\lambda_a(L)} P_a(L)_{\beta\alpha}, \quad (30)$$

where

$$P_a(L)_{\beta\alpha} = \frac{(\lambda_a^2 + c_1)\delta_{\beta\alpha} + \lambda_a \tilde{T}_{\beta\alpha} + (\tilde{T}^2)_{\beta\alpha}}{3\lambda_a^2 + c_1} \quad (31)$$

is the matrix element of the projector $P_a(L)$. Here $\delta_{\alpha\beta}$ is Kronecker's delta. Note that $\tilde{T}_{\alpha\beta} = \tilde{T}_{\beta\alpha}$ and $(\tilde{T}^2)_{\alpha\beta} = (\tilde{T}^2)_{\beta\alpha}$. The transition probability $P_{\alpha\beta}$ for $\nu_\alpha \rightarrow \nu_\beta$ transition is defined as the absolute value squared of the probability amplitude $A_{\alpha\beta}$. Hence, the transition probabilities in matter are given by the formulas

$$\begin{aligned} P_{\alpha\beta} &= |A_{\alpha\beta}|^2 \\ &= \delta_{\alpha\beta} - 4 \sum_{a=1}^3 \sum_{\substack{b=1 \\ a < b}}^3 P_a(L)_{\beta\alpha} P_b(L)_{\beta\alpha} \sin^2 \tilde{x}_{ab}, \\ \alpha, \beta &= e, \mu, \tau, \end{aligned} \quad (32)$$

where $\tilde{x}_{ab} \equiv (\lambda_a(L) - \lambda_b(L))L/2$.

6 Applications and discussion

The main results of our analysis are given by the evolution operator for the neutrinos when passing through matter with varying matter density in the ‘‘semi-classical approximation’’, (16), and the corresponding expressions for the transition amplitudes in (30) and the transition probabilities in (32), all expressed as finite sums of simple functions in the matrix elements of \mathcal{H}_f (or \mathcal{H}_m) and integrals involving $A(r)$, the varying matter density.

As applications, we have calculated the transition probability $P_{\mu e}$ for neutrino oscillations for different matter density profiles. Our calculations compare two different cases.

(1) An ‘‘exact’’ numerical evolution operator method based on the product of N evolution operators using

$$\begin{aligned} U_f(L) &= U_f(r_N - r_{N-1}) U_f(r_{N-1} - r_{N-2}) \dots \\ &\dots U_f(r_2 - r_1) U_f(r_1 - r_0), \end{aligned} \quad (33)$$

with the formula (8) used for each step with the appropriate matter density; and

(2) The semi-classical approximation method based on one single evolution operator using

$$U_f(L) = \bar{\phi} U e^{-iL\bar{T}} U^{-1}. \quad (34)$$

In all our examples discussed below, we have used the earth center crossing neutrino traveling path length, except for the last example in which we discuss the sun.

Let $R_\oplus \simeq 6371$ km be the radius of the earth and $r_\oplus \simeq 3486$ km be the radius of the core with this approximation and in a numerical simulation based on (9) with a step length of $L/N = 2R_\oplus/100 = 127.42$ km. The thickness of the mantle is then $R_\oplus - r_\oplus \simeq 2885$ km with the matter density parameter $A_1 = A_{\text{mantle}} \simeq 1.70 \cdot 10^{-13}$ eV ($\rho_1 = \rho_{\text{mantle}} \simeq 4.5$ g/cm³), whereas the matter density parameter of the core is $A_2 = A_{\text{core}} \simeq 4.35 \cdot 10^{-13}$ eV ($\rho_2 = \rho_{\text{core}} \simeq 11.5$ g/cm³).

Neutrinos traversing the earth towards a detector close to the surface of the earth, pass through the matter of varying density $A(r)$ where the distances L_i , $i = 1, 2$, are functions of the nadir angle h , where $h \equiv \pi - \theta_z$, θ_z being the zenith angle. As h varies from 0 to $\pi/2$, the cord $L = L(h)$ of the neutrino passage through earth becomes shorter and shorter. At an angle larger than $h_0 = \arcsin(r_\oplus/R_\oplus) \simeq 33.17^\circ$, the distance $L_2 = 0$, and the neutrinos no longer traverse the core.

The mass squared differences ($\Delta M^2 \equiv \Delta m_{32}^2$ and $\Delta m^2 \equiv \Delta m_{21}^2$) and the vacuum mixing angles ($\theta_1, \theta_2, \theta_3$) used here are chosen to correspond to those obtained from analyses of various neutrino oscillation data. We have taken

$$\begin{aligned} \Delta M^2 &= 3.2 \cdot 10^{-3} \text{eV}^2, \quad \Delta m^2 = 0, \quad \theta_1 = 45^\circ, \\ \theta_2 &= 5^\circ, \quad \theta_3 = 45^\circ. \end{aligned}$$

The values of ΔM^2 and θ_1 are governed by atmospheric neutrino data [27] and the values of Δm^2 and θ_3 (LMA) by solar neutrino data [28], where LMA stands for

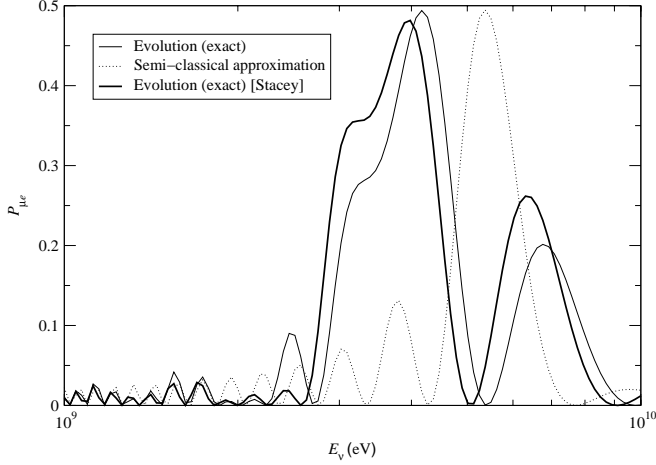


Fig. 1. The transition probability $P_{\mu e}$ as a function of the neutrino energy E_ν for the mantle–core–mantle step function approximation of the earth’s matter density profile. The mean matter density of the mantle and the core were chosen to be $\rho_{\text{mantle}} = 4.5 \text{ g/cm}^3$ ($A_{\text{mantle}} \simeq 1.7 \cdot 10^{-13} \text{ eV}$, $L_{\text{mantle}} = 2885 \text{ km}$) and $\rho_{\text{core}} = 11.5 \text{ g/cm}^3$ ($A_{\text{core}} \simeq 4.4 \cdot 10^{-13} \text{ eV}$, $L_{\text{core}} = 6972 \text{ km}$), respectively. Parameter values: $h = 0$, $\theta_1 = 45^\circ$, $\theta_2 = 5^\circ$, $\theta_3 = 45^\circ$, $\Delta m^2 = 0$, and $\Delta M^2 = 3.2 \cdot 10^{-3} \text{ eV}^2$

large mixing angle (matter) solution. The value of θ_2 is below the CHOOZ upper bound, which is $\sin^2 2\theta_2 = 0.10$ [29]. These choices are the most optimistic ones for obtaining any effects in long baseline (LBL) experiments from the sub-leading Δm^2 scale [30]. We should mention though, that these data are taken from two neutrino flavor model analyses.

As a first example, we have investigated the earth’s matter density profile using the published Stacey model for the earth’s matter density profile [26]. The resulting curves of the (exact) numerical evolution operator method for a mantle–core–mantle step function approximation of the earth’s matter density profile, the semi-classical approximation method, and for reference the (exact) numerical evolution operator method of the earth’s matter density profile are shown in Fig. 1. It has earlier been found by Freund and Ohlsson [17] that a mantle–core–mantle step function approximation of the earth’s matter density profile is a good approximation (even in a three neutrino scenario). The numerical evolution operator method results were carried out using $N = 100$, i.e., they consist of a product of 100 evolutions with different constant matter densities for each evolution step, whereas the semi-classical approximation method result was obtained with just one single evolution with the average matter density of the earth’s matter density profile \bar{A}_\oplus ($\bar{\rho}_\oplus \simeq 7.8 \text{ g/cm}^3$), which is also the reason why the semi-classical approximation curve only has got one resonance peak at $E_\nu = \bar{E}_{\nu,\oplus} \simeq 5.4 \cdot 10^9 \text{ eV}$. This peak of course lies in between the two resonance peaks (ideally at $E_\nu = E_{\nu,\text{core}} \simeq 3.7 \cdot 10^9 \text{ eV}$ and $E_\nu = E_{\nu,\text{mantle}} \simeq 9.4 \cdot 10^9 \text{ eV}$) of the exact numerical evolution calculation, since $A_{\text{mantle}} \leq \bar{A}_\oplus \leq A_{\text{core}}$.

In Figs. 2 and 3, we have used two different step function matter density profiles.

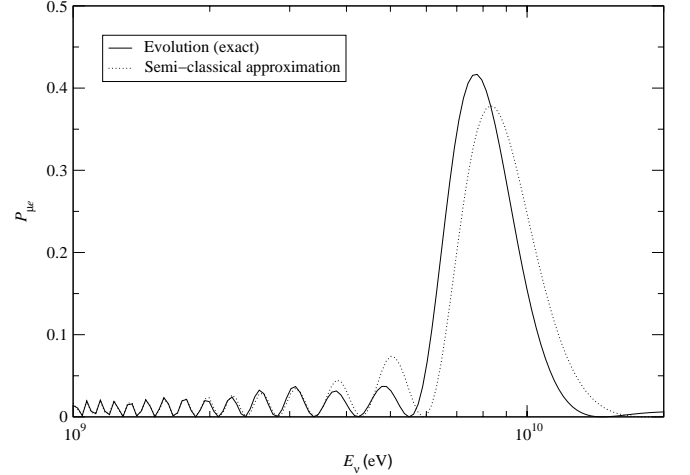


Fig. 2. The transition probability $P_{\mu e}$ as a function of the neutrino energy E_ν for a step function matter density profile with $\rho_1 = 4.5 \text{ g/cm}^3$ ($A_1 \simeq 1.7 \cdot 10^{-13} \text{ eV}$, $L_1 = 2885 \text{ km}$) and $\rho_2 = 5.5 \text{ g/cm}^3$ ($A_2 \simeq 2.1 \cdot 10^{-13} \text{ eV}$, $L_2 = 6972 \text{ km}$). Parameter values: $h = 0$, $\theta_1 = 45^\circ$, $\theta_2 = 5^\circ$, $\theta_3 = 45^\circ$, $\Delta m^2 = 0$, and $\Delta M^2 = 3.2 \cdot 10^{-3} \text{ eV}^2$

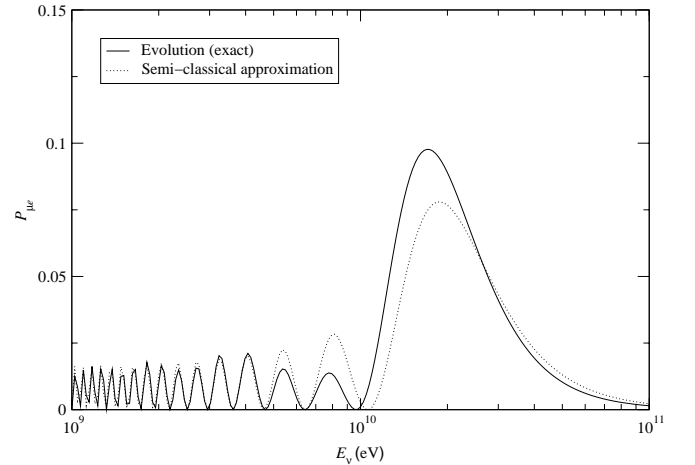


Fig. 3. The transition probability $P_{\mu e}$ as a function of the neutrino energy E_ν for a step function matter density profile with $\rho_1 = 1 \text{ g/cm}^3$ ($A_1 \simeq 3.8 \cdot 10^{-14} \text{ eV}$, $L_1 = 2885 \text{ km}$) and $\rho_2 = 2 \text{ g/cm}^3$ ($A_2 \simeq 7.6 \cdot 10^{-14} \text{ eV}$, $L_2 = 6972 \text{ km}$). Parameter values: $h = 0$, $\theta_1 = 45^\circ$, $\theta_2 = 5^\circ$, $\theta_3 = 45^\circ$, $\Delta m^2 = 0$, and $\Delta M^2 = 3.2 \cdot 10^{-3} \text{ eV}^2$

There appear no double peaks in these figures even though the step function matter density profiles consist of two different A_k ’s. Furthermore, in Figs. 2 and 3, the differences between the values of the A_1 ’s and A_2 ’s are the same. The step function matter density profile in Fig. 2 could simulate the earth’s matter density profile if the earth has a core, which is much less dense than has been found by geophysics. Note that the absolute error between the two curves in Fig. 2 is larger than in Fig. 3, whereas the relative error of the curves in Fig. 3 is larger than in Fig. 2.

Next, in Figs. 4 and 5, we have studied constant matter density profiles.

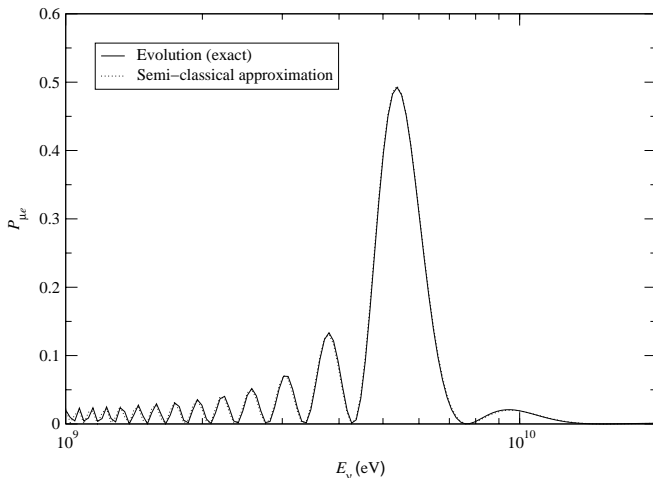


Fig. 4. The transition probability $P_{\mu e}$ as a function of the neutrino energy E_ν for a constant matter density profile with $\rho = 7.8 \text{ g/cm}^3$ ($A \simeq 3.0 \cdot 10^{-13} \text{ eV}$, $L = 12742 \text{ km}$). Parameter values: $h = 0$, $\theta_1 = 45^\circ$, $\theta_2 = 5^\circ$, $\theta_3 = 45^\circ$, $\Delta m^2 = 0$, and $\Delta M^2 = 3.2 \cdot 10^{-3} \text{ eV}^2$

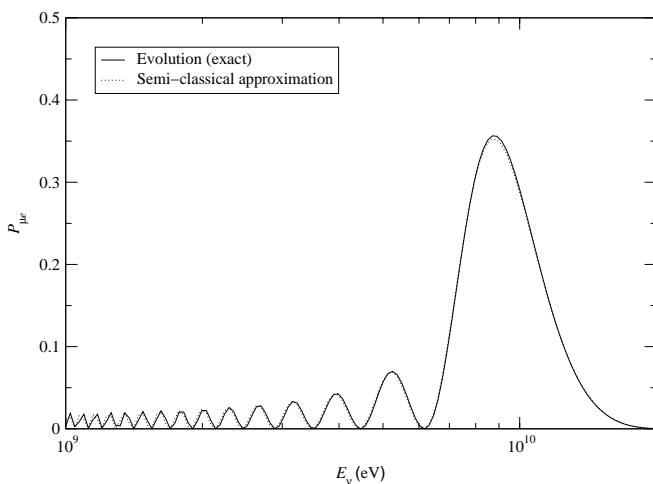


Fig. 5. The transition probability $P_{\mu e}$ as a function of the neutrino energy E_ν for a constant matter density profile with $\rho = 4.5 \text{ g/cm}^3$ ($A \simeq 1.7 \cdot 10^{-13} \text{ eV}$, $L = 12742 \text{ km}$). Parameter values: $h = 0$, $\theta_1 = 45^\circ$, $\theta_2 = 5^\circ$, $\theta_3 = 45^\circ$, $\Delta m^2 = 0$, and $\Delta M^2 = 3.2 \cdot 10^{-3} \text{ eV}^2$

The constant matter density used in Fig. 4 is the average density of the earth. The curves in this figure could be compared with the dotted curve in Fig. 1. In Fig. 5, the constant matter density was chosen to be equal to the average density in the mantle of the earth. In both these figures, the semi-classical approximation method gives an excellent agreement with the exact numerical evolution operator method as it should, since in the case of constant matter density $\bar{A} = A = \text{const.}$, which means that the two methods are equivalent. Thus, the very small deviations seen in the figures are only due to numerics.

Then, in Figs. 6 and 7, we discuss linear matter density profiles.

The parameter B used in Fig. 6 is larger than that in Fig. 7. The smaller B is the better the agreement between

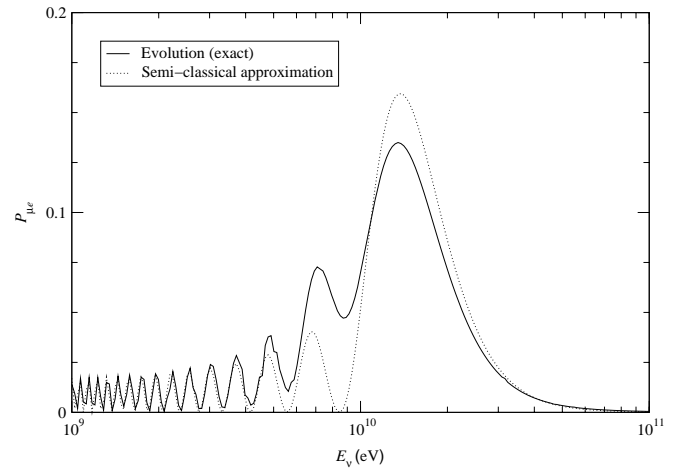


Fig. 6. The transition probability $P_{\mu e}$ as a function of the neutrino energy E_ν for a linear matter density profile with $A = 0$ and $BL \simeq 3.8 \cdot 10^{-13} \text{ eV}$ (corresponding to $\rho = 5 \text{ g/cm}^3$ and $L = 12742 \text{ km}$ if $A = BL/2$). Parameter values: $h = 0$, $\theta_1 = 45^\circ$, $\theta_2 = 5^\circ$, $\theta_3 = 45^\circ$, $\Delta m^2 = 0$, and $\Delta M^2 = 3.2 \cdot 10^{-3} \text{ eV}^2$

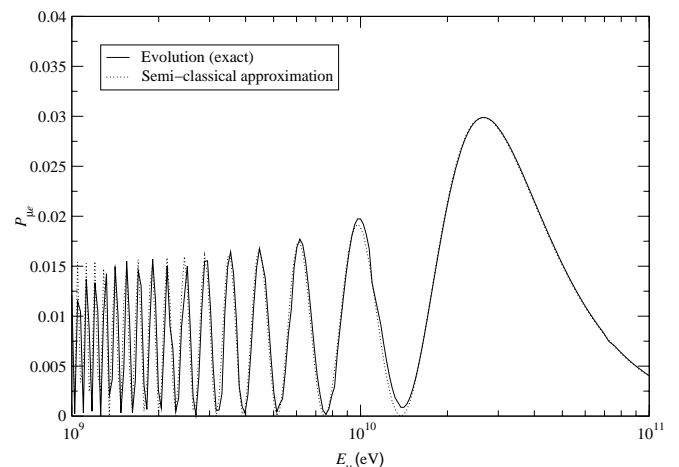


Fig. 7. The transition probability $P_{\mu e}$ as a function of the neutrino energy E_ν for a linear matter density profile with $A = 0$ and $BL \simeq 7.6 \cdot 10^{-14} \text{ eV}$ (corresponding to $\rho = 1 \text{ g/cm}^3$ and $L = 12742 \text{ km}$ if $A = BL/2$). Parameter values: $h = 0$, $\theta_1 = 45^\circ$, $\theta_2 = 5^\circ$, $\theta_3 = 45^\circ$, $\Delta m^2 = 0$, and $\Delta M^2 = 3.2 \cdot 10^{-3} \text{ eV}^2$

the numerical evolution operator method and the semi-classical approximation method becomes. However, linear matter density profiles only have theoretical interest, since they are not to be found in Nature at least at large distance scales. They could, however, be used on shorter distance scales though, e.g., LBL experiments like K2K, MINOS, and CERN-LNGS [31], where the neutrinos traverse the earth mantle with cord-like paths.

Finally, in Fig. 8, we investigated the sun's matter density profile, which is an exponentially decreasing matter density profile. The semi-classical approximation method does not work as well in this case as for step function, con-

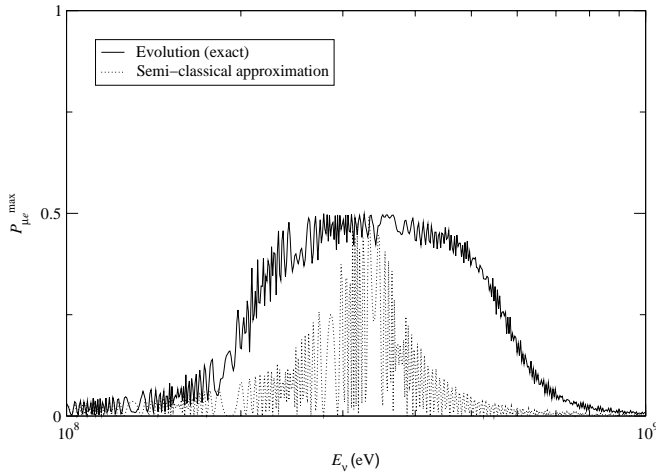


Fig. 8. The transition probability $P_{\mu e}$ as a function of the neutrino energy E_{ν} for the exponentially decreasing matter density profile of the sun with $\rho_{\odot}(r) = \rho_{\odot}(0)e^{-r/r_0}$, where $\rho_{\odot}(0) = 200 \text{ g/cm}^3$, $r_0 = R_{\odot}/10.54 \simeq 66000 \text{ km}$, and $R_{\odot} \simeq 6.96 \cdot 10^8 \text{ m}$ [32]. Parameter values: $\theta_1 = 45^\circ$, $\theta_2 = 5^\circ$, $\theta_3 = 45^\circ$, $\Delta m^2 = 0$, and $\Delta M^2 = 3.2 \cdot 10^{-3} \text{ eV}^2$

stant, and linear matter density profiles, since this matter density profile is varying too quickly³.

In conclusion, the semi-classical approximation will be a good approximation for some types of matter density profiles. In certain cases, of slowly varying matter density, it is even an excellent approximation. The major advantage of the semi-classical approximation method as compared to the exact numerical evolution operator method is that we only need to calculate one single evolution operator for one single average matter density, the average matter density parameter of the considered matter density profile $\bar{A}(L)$, i.e., we can make the replacement

$$U_f(L) = \underbrace{\prod_{i=1}^n U_f(L_i, A_i)}_{n \text{ operators}} \rightarrow U_f(L) = \underbrace{\bar{\phi} e^{-iLT}}_{\text{one operator}}.$$

Acknowledgements. We would like to thank Martin Freund for useful comments. This work was supported by the Swedish Foundation for International Cooperation in Research and Higher Education (STINT) [T.O.], the Wenner-Gren Foundations [T.O.], the ‘‘Sonderforschungsbereich 375 f ur Astro-Teilchenphysik der Deutschen Forschungsgemeinschaft’’ [T.O.], and the Swedish Natural Science Research Council (NFR), Contract No. F 650-19981428/2000 [H.S.].

³ A remark about the neutrino energy interval shown in Fig. 8 is in place. Solar neutrinos have energies of the order of 0.1 MeV–10 MeV, i.e., energies much smaller than what is shown in Fig. 8. However, the resonance energy due to the large mass squared difference $\Delta M^2 = 3.2 \cdot 10^{-3} \text{ eV}^2$ is given in Fig. 8. Thus, the neutrino energy interval shown in Fig. 8 is only of theoretical interest and the figure shows how well the semi-classical approximation works in the region where the transition probability $P_{\mu e}$ changes most

References

1. T. Ohlsson, H. Snellman, J. Math. Phys. **41**, 2768 (2000), hep-ph/9910546; **42**, 2345 (E) (2001)
2. T. Ohlsson, H. Snellman, Phys. Lett. B **474**, 153 (2000), hep-ph/9912295; **480**, 419(E) (2000)
3. S.P. Mikheyev, A.Yu. Smirnov, Yad. Fiz. **42**, 1441 (1985) [Sov. J. Nucl. Phys. **42**, 913 (1985)]; Nuovo Cimento C **9**, 17 (1986)
4. L. Wolfenstein, Phys. Rev. D **17**, 2369 (1978); **20**, 2634 (1979)
5. V. Barger, K. Whisnant, S. Pakvasa, R.J.N. Phillips, Phys. Rev. D **22**, 2718 (1980)
6. C.W. Kim, W.K. Sze, Phys. Rev. D **35**, 1404 (1987)
7. H.W. Zaglauer, K.H. Schwarzer, Z. Phys. C **40**, 273 (1988)
8. T.K. Kuo, J. Pantaleone, Phys. Rev. Lett. **57**, 1805 (1986)
9. A.S. Joshipura, M.V.N. Murthy, Phys. Rev. D **37**, 1374 (1988)
10. S. Toshev, Phys. Lett. B **185**, 177 (1987); **192**, 478(E) (1987); S.T. Petcov, S. Toshev, Phys. Lett. B **187**, 120 (1987); S.T. Petcov, Phys. Lett. B **200**, 373 (1988)
11. J.C. D’Olivo, J.A. Oteo, Phys. Rev. D **54**, 1187 (1996)
12. G.L. Fogli, E. Lisi, D. Montanino, Phys. Rev. D **49**, 3626 (1994); G.L. Fogli, E. Lisi, D. Montanino, Phys. Rev. D **54**, 2048 (1996), hep-ph/9605273; G.L. Fogli, E. Lisi, D. Montanino, G. Scioscia, Phys. Rev. D **55**, 4385 (1997), hep-ph/9607251; G.L. Fogli, E. Lisi, A. Marrone, G. Scioscia, Phys. Rev. D **59**, 033001 (1999), hep-ph/9808205
13. A. Nicolaidis, Phys. Lett. B **200**, 553 (1988)
14. C. Giunti, C.W. Kim, M. Monteno, Nucl. Phys. B **521**, 3 (1998), hep-ph/9709439
15. Q.Y. Liu, A.Yu. Smirnov, Nucl. Phys. B **524**, 505 (1998), hep-ph/9712493; Q.Y. Liu, S.P. Mikheyev, A.Yu. Smirnov, Phys. Lett. B **440**, 319 (1998), hep-ph/9803415; P. Lipari, M. Lusignoli, Phys. Rev. D **58**, 073005 (1998), hep-ph/9803440; E.Kh. Akhmedov, Nucl. Phys. B **538**, 25 (1999), hep-ph/9805272; E.Kh. Akhmedov, A. Dighe, P. Lipari, A.Yu. Smirnov, Nucl. Phys. B **542**, 3 (1999), hep-ph/9808270; E.Kh. Akhmedov, hep-ph/9903302; Pramana **54**, 47 (2000), hep-ph/9907435
16. S.T. Petcov, Phys. Lett. B **434**, 321 (1998), hep-ph/9805262; **444**, 584(E) (1998); M. Chizhov, M. Maris, S.T. Petcov, hep-ph/9810501; M.V. Chizhov, S.T. Petcov, Phys. Rev. Lett. **83**, 1096 (1999), hep-ph/9903399; Phys. Rev. D **63**, 073003 (2001), hep-ph/9903424
17. M. Freund, T. Ohlsson, Mod. Phys. Lett. A **15**, 867 (2000), hep-ph/9909501
18. I. Mocioiu, R. Shrock, Phys. Rev. D **62**, 053017 (2000), hep-ph/0002149
19. S.T. Petcov, Phys. Lett. B **191**, 299 (1987)
20. H. Lehmann, P. Osland, T.T. Wu, hep-ph/0006213
21. P. Osland, T.T. Wu, Phys. Rev. D **62**, 013008 (2000), hep-ph/9912540
22. A.B. Balantekin, J.F. Beacom, Phys. Rev. D **54**, 6323 (1996), hep-ph/9606353
23. P.M. Fishbane, S.G. Gasiorowicz, hep-ph/0012230; P.M. Fishbane, P. Kaus, hep-ph/0101013
24. C.W. Kim, A. Pevsner, Neutrinos in physics and astrophysics (Harwood Academic, Chur, Switzerland 1993)
25. Particle Data Group, D.E. Groom et al., Review of Particle Physics, Eur. Phys. J. C **15**, 1 (2000), pdg.lbl.gov
26. F.D. Stacey, Physics of the earth (Wiley, 1977), 2nd edition

27. K. Scholberg [Super-Kamiokande Collaboration], hep-ex/9905016
28. J.N. Bahcall, P.I. Krastev, A.Yu. Smirnov, Phys. Rev. D **58**, 096016 (1998), hep-ph/9807216; **60**, 093001 (1999), hep-ph/9905220; hep-ph/0103179
29. CHOOZ Collaboration, M. Apollonio et al., Phys. Lett. B **420**, 397 (1998), hep-ex/9711002; Phys. Lett. B **466**, 415 (1999), hep-ex/9907037
30. V. Barger, S. Geer, R. Raja, K. Whisnant, Phys. Rev. D **62**, 013004 (2000), hep-ph/9911524
31. CERN-LNGS Collaboration, P. Picchi, F. Pietropaolo, Nucl. Phys. B (Proc. Suppl.) **77**, 187 (1999); S.G. Wojcicki, Nucl. Phys. B (Proc. Suppl.) **77**, 182 (1999); K2K Collaboration, K. Nishikawa, Nucl. Phys. B (Proc. Suppl.) **77**, 198 (1999)
32. J.N. Bahcall, Neutrino astrophysics (Cambridge University Press, Cambridge 1989); J.N. Bahcall, M.H. Pinsonneault, S. Basu, Astrophys. J. (to be published), astro-ph/0010346